Eur. J. Mineral.
1995, 7, 1251-1272

This paper has been presented at the I.M.A.
meeting in Pisa (September 1994)

Archean high-pressure metamorphism in the western Canadian Shield

DAVID R. SNOEYENBOS[1], MICHAEL L. WILLIAMS[1] and SIMON HANMER[2]

[1] Department of Geosciences, University of Massachusetts, Amherst, Massachusetts, 01003, U.S.A.

[2] Continental Geoscience Division, Geological Survey of Canada, 601 Booth St., Ottawa, Ontario, K1A 0E8, Canada

Abstract: The upper deck of the 3.2-2.6 Ga East Athabasca mylonite triangle, northern Saskatchewan, Canada consists predominantly of crustal rocks metamorphosed at conditions exceeding 15 kbar and 1000°C. Mylonitic quartzofeldspathic gneisses and gneiss-hosted metabasite alike record these conditions. Temperature is constrained to at least 1000°C by homogenization thermometry of ternary feldspars in the felsic gneisses and by garnet-clinopyroxene exchange thermometry in mafic rocks. Minimum pressure of 15 kbar is indicated by the presence of matrix kyanite in association with the high-temperature feldspars. Primary corundum in certain garnet-clinopyroxenites also indicates pressure of at least 15 kbar.

Unusual mineral compositions such as Ti-rich muscovite, Cr-bearing kyanite, and possible zircon exsolution from rutile are found in several locations. Oriented rutile needles in garnet, interpreted as exsolution, are pervasive.

The upper deck is a discrete metamorphic terrane, 400 km^2 in area and 10 km in thickness. Elevation of this terrane into juxtaposition and fusion with granulite-facies lower crustal mylonites occurred within a 2.6 Ga intracontinental strike-slip shear zone. The upper deck is one of the very few high-pressure crustal metamorphic provinces known in the Americas and at 2.6 Ga it is among the oldest such, worldwide.

Key-words: Archean, Canada, thermobarometry, high-pressure metamorphism.

Introduction

In recent years metamorphic petrology has been invigorated and in many ways transformed by a succession of discoveries of extremely high temperature and pressure metamorphic terranes. With the recognition of these terranes has come the problem of how such rocks, particularly the highest temperature ones, can be returned to the upper crust without complete resetting of mineral equilibria. These terranes test our understanding of the dynamic controls on metamorphism.

Here we introduce a crustal metamorphic terrane, the 'upper deck' of the East Athabasca mylonite triangle, northern Saskatchewan, Canada (Hanmer, 1994). This extremely high grade metamorphic terrane stands well away from others not in pressure and temperature, which at minima of 15 kbar and 1000°C are unusual but not unique, but in geographical, temporal and tectonic respects. Lodged in a 3.2-2.6 Ga intracontinental transcurrent shear zone in western Laurentia, this terrane is the first very high pressure crustal terrane known in the Americas, is among the oldest such known worldwide, and occurs in a novel and problematic tectonic setting. Further, among extremely high grade metamorphic terranes the upper deck may also be unusual in that the rocks are well exposed, fresh and generally show limited retrograde metamorphic effects outside of the granulite facies across their 400 km^2 area.

0935-1221/95/0007-1251 $ 5.50

This contribution is intended as a preliminary description of the high pressure petrology of the upper deck. We therefore focus on general lithologic properties, concentrating on examples of those mineral assemblages, exchange equilibria and mineral compositions that constrain the P-T minima. The retrograde P-T path, available in some detail from well preserved multiple generations of symplectitic and coronitic reaction textures, will be considered elsewhere.

Geological setting

The western Canadian Shield is divided into Archean Rae and Hearne crustal provinces by a *ca.* 3000 km long linear gravity anomaly (Thomas *et al.*, 1988), referred to as the Snowbird tectonic zone (Hoffman, 1988). At the east end of Lake Athabasca (Fig. 1), northern Saskatchewan, the Snowbird tectonic zone widens to form a 125 x 80 x 75 km domain of hetero-

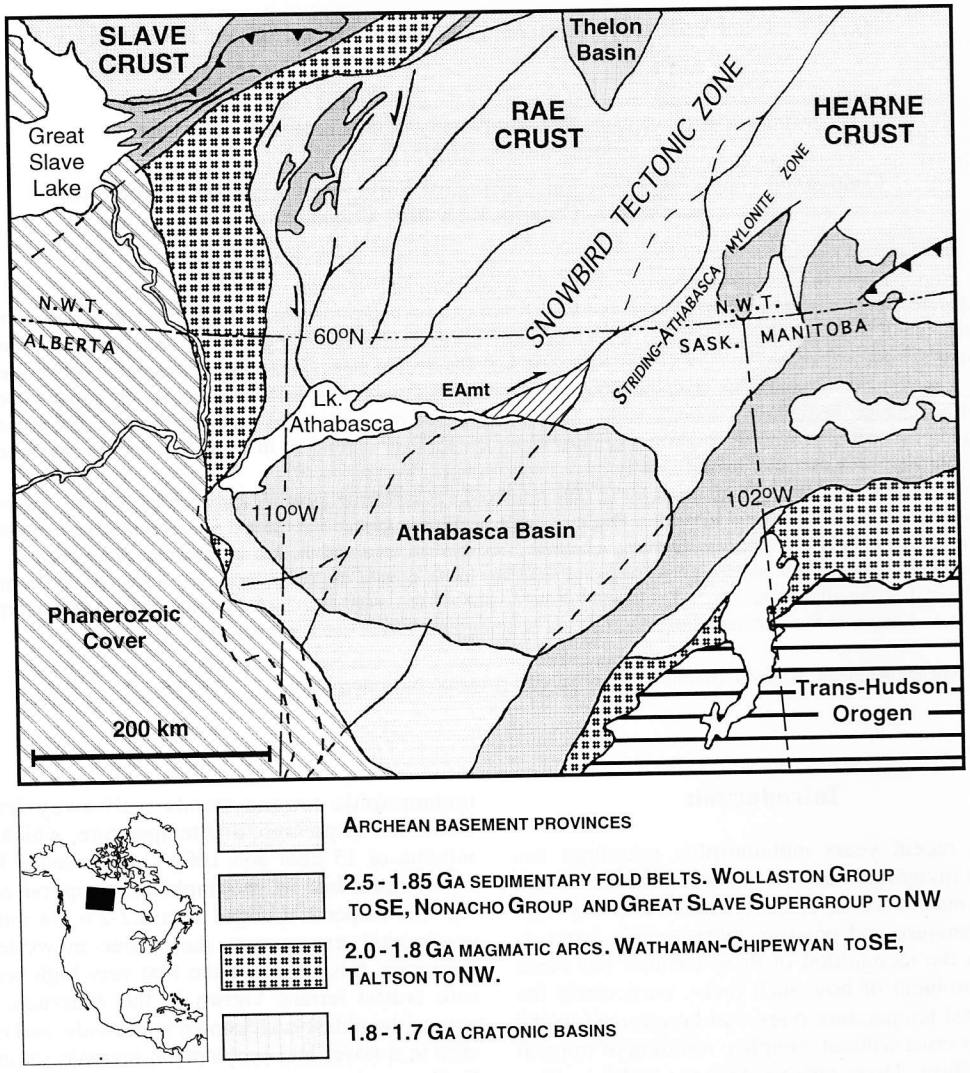

Fig. 1. Map of western Laurentia showing the regional setting of the Striding-Athabasca mylonite zone and the East Athabasca mylonite triangle (EAmt). The Snowbird tectonic zone is between the Archean Rae and Hearne provinces of the Canadian Shield. Units within the 1.9-1.8 Ga Trans-Hudson orogen are not distinguished. The dashed contacts beneath post-tectonic Proterozoic and Phanerozoic sediments are inferred from aeromagnetic and gravimetric data. Adapted from Hoffman (1989).

geneous lower-crustal mylonites, the Middle to Late Archean East Athabasca mylonite triangle (EAmt; Hanmer, 1994; Hanmer *et al.*, 1994).

The EAmt is the southwestern segment of the sinuous, dextral transpressive Striding-Athabasca mylonite zone, which is characterized by granulite-facies mineral assemblages (Hanmer *et al.*, 1995). This lower crustal mylonite zone is bounded by cratonic mid-crustal gneisses of the Rae Province (northwest) and by the mid- to upper-crustal greenstones of the Rankin-Ennedai Belt in the Hearne Province (southeast). To the south the mylonites are covered by Lake Athabasca and the sandstones of the Middle Proterozoic Athabasca Basin (1.7 Ga: Cumming & Krstic, 1992). Aeromagnetic data show that the EAmt is at the northeastern tip of a *ca.* 100 x 300 km lenticular body of possibly similar rocks, which is the southwesternmost and largest of a chain of three such bodies or lozenges within the Snowbird tectonic zone extending northeast into the Northwest Territories (Hanmer *et al.*, 1995).

The EAmt is a region of considerable lithologic complexity and intense polyphase deformation that has resulted nonetheless in a remarkably simple gross structure (Fig. 2). Three general structural and metamorphic domains are recognized.

The northwestern parts of the triangle are lithologically heterogeneous granulite-facies mylonites (800-900°C, 10 kbar) with various plutonic and sedimentary protoliths. Foliation is subvertical, striking northeast with a gently southwest-plunging extension lineation associated with intense dextral shearing at 2.62-2.60 Ga. Some reactivation may have occurred in the Early Proterozoic, *ca.* 1.9-1.8 Ga, perhaps associated with the Trans-Hudson orogeny.

The eastern parts consist largely of the mylonitized tonalitic Chipman batholith, likewise granulite-facies (850-900°C, 10 kbar). Here, abundant tonalitic melt is interpreted to have been generated by vapor-absent melting of MORB-composition hornblendite dikes invading the lowermost crust (Williams *et al.*, 1995). Two

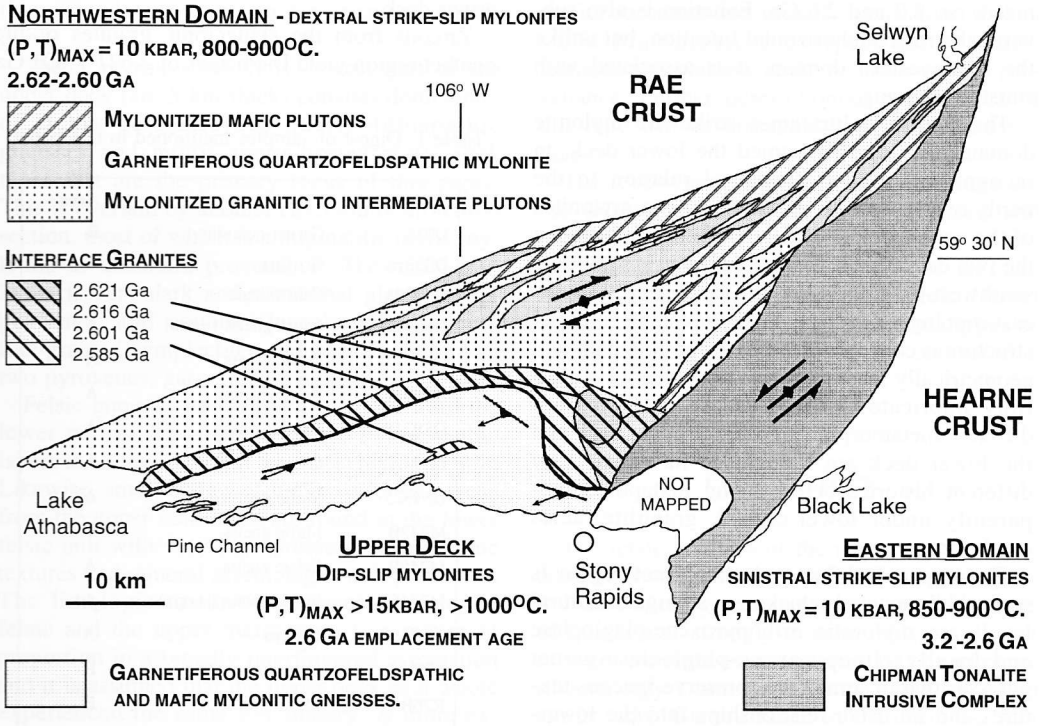

Fig. 2. Generalized lithologic and tectonic elements of the East Athabasca mylonite triangle. For a more detailed presentation see Hanmer (1994).

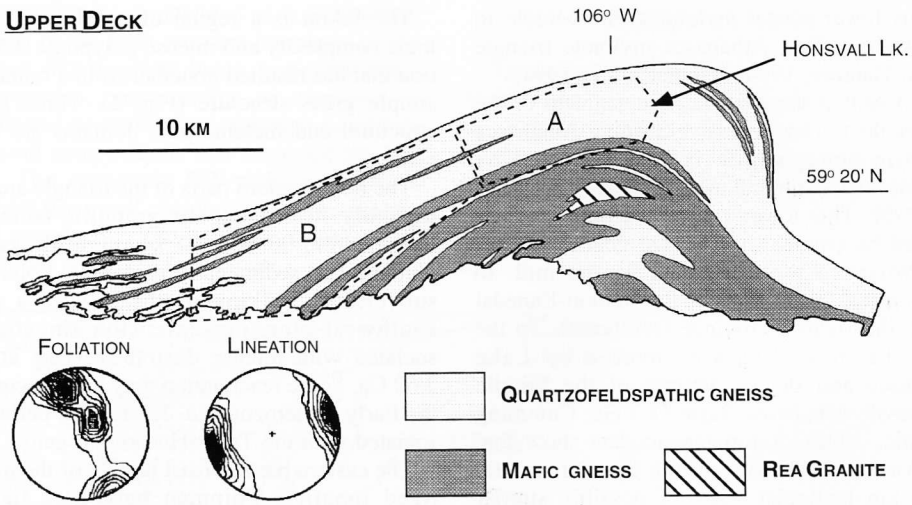

Fig. 3. Detail map of the upper deck showing its general division into quartzofeldspathic and mafic mylonitic gneisses. Areas 'A' and 'B' are source areas for samples mentioned in the text and indexed in Table 1.

intrusive and deformational periods are recognized, *ca*. 3.2 and 2.6 Ga. Foliation is also subvertical with a subhorizontal lineation, but unlike the northwestern domain, it is associated with sinistral shearing.

The two granulite-facies strike-slip mylonite domains are together named the lower deck, in recognition of their structural relation to the partly overlying high-pressure dip-slip mylonites of the upper deck (Fig. 3). The interface between the two decks is curved, such that it is shallowly southwest-dipping in the east, and steeply southeast-dipping to vertical in the west. Its internal structure is concordant to the lower boundary and geometrically resembles a folded sheet or a multiply imbricate thrust. Because of their very different metamorphic grades, the upper deck and the lower deck are thought to have had very different histories before being juxtaposed, apparently under lower-crustal, granulite-facies conditions.

The upper deck/lower deck contact region is several kilometers in thickness. At high structural levels are mylonitic orthopyroxene-plagioclase and locally clinopyroxene-plagioclase-garnet gneisses that in some cases preserve igneous textures and intrusive relationships into the lowermost part of the upper deck. Lower in the contact region is a suite of granites most likely related to the overhead emplacement and adjustment of the dry and extremely high temperature rocks of the upper deck.

Zircons from the syntectonic granites of the contact region yield U-Pb ages of 2.621-2.601 Ga

Table 1. Digest of samples mentioned in this paper.

Specimen #	Type	Area
D016	Garnet-quartzite	B
D033E1	Grt-Cpx	A
DS9305	Calc-silicate	A
DS9311	Felsic gneiss (+crn)	A
DS9315	Felsic gneiss	A
DS9317	Felsic gneiss	A
DS9318	Felsic gneiss	A
DS9322	Grt-cpx	A
DS9325	Mafic gneiss	A
M242B	Mafic gneiss	B
M249B	Felsic gneiss	A
M2315	Felsic gneiss (+opx)	A
M2319A	Grt-cpx	A
M2506	Garnet-quartzite	B
R76B	Mafic gneiss	B
R77	Felsic gneiss (+crn)	B

Areas 'A' and 'B' refer to the regions shown in Fig. 3.

(Hanmer *et al.*, 1994). Further geochronologic constraints are provided by the 2.585 Ga Rea Granite which is a late syndeformational pluton within the upper deck, and by similar cooling ages from monazite in adjacent felsic gneisses. The age of juxtaposition of the upper and lower decks is therefore 2.62-2.59 Ga and this is understood as a minimum for the age of the high-pressure metamorphism.

The upper deck

The upper deck is an arcuate terrane approximately 400 km^2 in area and 10 km in thickness assuming continuation at depth of mappable structures (Hanmer *et al.*, 1992). The surface is rugged, with ridges tens of kilometers long marking the trace of high-pressure granulite-facies mylonites dipping gently to steeply southwards. A shallowly WSW-plunging mineral lineation is found in both highest-grade and overprinting granulite-facies mineral assemblages and is therefore interpreted to have been developed continuously during uplift to lower-crustal conditions.

The northern, structurally lowest part of the upper deck (*ca.* 5 km thick) consists dominantly of richly garnetiferous quartzofeldspathic gneisses and minor gneiss-hosted mafic rock types that are the primary focus of this paper. This is overlain by another *ca.* 5 km of structural section, most of which is a migmatitic mafic mylonite of uncertain provenance. The mafic mylonite is very dark and somewhat glassy in appearance, and consists largely of extremely fine-grained symplectites and coronae involving two pyroxenes, garnet and plagioclase.

Felsic gneisses very similar to those from the lower part of the upper deck are found in thin layers at all levels within the mafic mylonite unit. Likewise, small bodies of mafic rocks like those from the upper mafic unit are found in the lower felsic unit with very high pressure metamorphic textures and mineral assemblages well preserved. The lithologic distinction between the lower felsic and the upper mafic units is a matter of proportion in a broadly interfingered association and it is assumed that the upper deck as a whole experienced the same P-T history. A more extensive granulite-facies overprinting has affected the upper unit. Further discussion of the mafic mylonite from the higher structural levels of the upper deck is beyond the scope of this paper.

Locally the felsic gneisses host other rock types including garnet quartzite, garnet orthopyroxenite, garnet clinopyroxenite and corundum- and kyanite-bearing garnet clinopyroxenite. Rare, thin calc-silicate bands contain clinopyroxene, calcite and Ca-Fe garnet. Nodules and bands of garnetite 5-15 cm thick contain lavender corundum megacrysts with accessory kyanite and spinel. The presence of quartz-rich rocks and rare calc-silicates in a package of mostly quartzofeldspathic gneisses encourages the interpretation that this part of the upper deck is of supracrustal, largely metasedimentary origin.

Included mafic rocks can retain igneous or deformational textures, overprinted by extensive development of coronitic garnet in plagioclase domains, and by garnet and clinopyroxene coronae around ductilely-deformed orthopyroxene megacrysts. Associated minerals in rocks of this type are Mg-rich ilmenite, Al-F-rich titanite and K-feldspar found as inclusions in coronitic garnet. The mineral assemblages, deformational textures and reaction textures in these mafic coronites are broadly consistent with a static high-pressure overprinting of mafic gneisses and plutonic rocks of lower-crustal provenance. Further description of mafic rocks of this type will be presented in another contribution.

The rock types that will be examined here are the felsic gneisses, both quartz-saturated and quartz-undersaturated varieties, and a peraluminous garnet-clinopyroxenite from Honsvall Lake in the northern part of the upper deck. Garnet compositions from these and other rock types of the upper deck are presented for comparative purposes in Fig. 4.

Felsic gneisses

The felsic gneisses of the upper deck are predominantly ribbon mylonites with abundant pink to lilac-colored garnets set in a matrix of ribbons of quartz and strongly ternary feldspar. Aspect ratios of the ribbons can be over 100:1 and many ribbons only 1 mm wide are traceable for 10-20 cm or more. Garnets range in size from 1-2 mm to several cm and typically comprise at least 20-30 % of the rock. Kyanite is found throughout the felsic gneisses both included in garnet and as

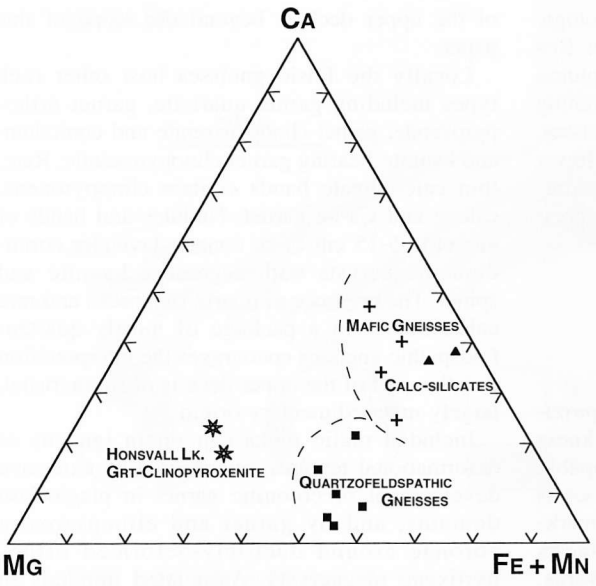

Fig. 4. Representative garnet compositions from various rock types of the upper deck. All garnets shown here are less than $Sp_{1.3}$. Garnets are from specimens DS9322, M2319A (eclogites); DS9315, M249B, R77, M2506, DS9308 (felsic gneiss); M242B, R76B, DS9325 (mafic gneiss); and DS9305 (calc-silicate).

a matrix phase. In the field, kyanite is visible as minute, intensely blue inclusions in garnet.

Quartz-saturated felsic gneisses are characterized by the assemblage garnet-quartz-ternary feldspar-kyanite-rutile, with common accessory zircon, monazite and chlorapatite. Relics of apparently higher-grade assemblages and unusual mineral compositions are found rarely in matrix but commonly as inclusions in garnet.

Phlogopite is found only as inclusions in garnet and in local retrograde associations with sillimanite and was evidently not part of the equilibrium assemblage at the highest grade. Discrete plagioclase is found as a syn- to post-deformational phase around garnet, kyanite and quartz. Plagioclase as a discrete phase is therefore also assigned a retrograde origin. Relic kyanite + quartz assemblages in calcic garnet with no primary plagioclase suggest that the anorthite molecule itself, even as it occurs in ternary feldspars, is only of retrograde origin (see later discussion).

The felsic gneisses range widely in their SiO_2 content. The varieties richest in quartz are more properly termed garnet-quartzites and most likely had a sedimentary protolith. The most volumetrically important varieties of the felsic gneiss contain 20-30 % modal quartz found as ribbons in matrix and as unstrained, up to 6 mm diameter spheroidal monocrystalline inclusions in garnet. Both included and matrix quartz typically contain oriented rutile needles. Quartz-absent varieties of the gneiss generally contain abundant corundum as *ca.* 1 cm crystals included in garnet and as small grains free in matrix, with accessory spinel and kyanite.

Garnet

The garnets of the felsic gneisses are notably Mg-Ca rich, up to $Py_{30}Gr_{20}$ and to Py_{43} at lower grossular content (Fig. 4). Spessartine content is very low and homogeneous at *ca.* Sp_1, probably not reflecting low whole-rock MnO contents but the diffusional homogenization of spessartine among all garnet crystals in very garnet-rich rocks. Cr_2O_3 is detectable but minor, less than 0.1 wt%. Na_2O, P_2O_5 and TiO_2 are generally at or near detection limits (Table 2).

A notable and distinctive characteristic of the garnets of the felsic gneisses is the widespread and abundant occurrence of fine haze of rutile needles in four specific orientations (Fig. 5). These are interpreted to have formed by exsolution and can readily be distinguished from sagenitic rutile (locally oriented rutile inclusions interpreted as overgrown biotite domains) by the consistency of orientation maintained across a centimeter or more of garnet. The needles are typically less than 2 μm in diameter and can be up to several hundred μm in length. The only

Table 2. Selected microprobe analyses of minerals from the felsic gneisses.

Spec.	M2506 Grt	M2506 Grt	DS9315 Grt	DS9315 Rt	DS9311 Ky	DS9311 Crn	DS9311 Spl	M2506 Phl	M2506 Ms
	high-Ca	low-Ca		lamella	incl.	incl.	incl.	incl.	matrix
P_2O_5	n.a.	0.06	0.06	n.a.	n.a.	n.a.	n.a.	n.a.	n.a.
SiO_2	39.74	39.03	38.70	0.03	37.46	0.04	0.04	37.89	47.52
TiO_2	n.a.	0.04	0.09	98.51	0.04	0.01	0.14	3.98	4.18
Al_2O_3	22.50	22.88	21.98	n.d.	59.92	98.56	57.49	16.68	30.36
Fe_2O_3	0.00	0.00	0.00	0.00	0.63	0.38	0.12	0.00	0.00
Cr_2O_3	n.a.	0.07	0.06	0.06	2.21	1.02	2.12	0.18	0.01
V_2O_3	n.a.	n.a.	n.a.	n.d.	0.22	0.04	0.36	n.a.	n.a.
ZnO	n.a.	n.a.	n.a.	n.a.	n.a.	n.a.	19.42	n.a.	n.a.
MgO	10.56	11.23	7.87	n.d.	0.02	0.02	4.89	17.85	1.99
FeO	21.83	25.22	22.83	0.76	0.00	0.00	15.96	9.15	0.67
MnO	0.49	0.32	0.34	n.d.	n.d.	0.01	n.d.	n.d.	n.d.
CaO	5.27	1.25	7.97	0.06	n.d.	n.d.	n.d.	n.d.	0.03
BaO	n.a.	n.a.	n.a.	n.a.	n.a.	n.a.	n.a.	0.56	0.33
Na_2O	n.a.	0.03	0.01	n.a.	n.a.	n.a.	n.a.	0.09	0.23
K_2O	n.a.	n.a.	n.a.	n.a.	n.a.	n.a.	n.a.	9.27	9.76
Total	100.39	100.13	99.91	99.42	100.50	100.08	100.54	95.65	95.08
/N ox.:	*12*	*12*	*12*	*2*	*5*	*3*	*4*	*11*	*11*
P	----	0.004	0.004	----	----	----	----	----	----
Si	2.993	2.960	2.972	0.001	1.015	0.001	0.001	2.743	3.165
Ti	----	0.002	0.005	0.989	0.001	----	0.003	0.217	0.209
Al	1.997	2.045	1.990	----	1.913	1.979	1.936	1.423	2.383
Fe^{3+}	----	----	----	----	0.013	0.005	0.003	----	----
Cr	----	0.004	0.003	0.001	0.047	0.014	0.048	0.010	----
V	----	----	----	----	0.005	0.001	0.008	----	----
Zn	----	----	----	----	----	----	0.410	----	----
Mg	1.186	1.269	0.901	----	0.001	----	0.208	1.927	0.198
Fe^{2+}	1.375	1.599	1.466	0.008	----	----	0.382	0.554	0.038
Mn	0.031	0.021	0.022	----	----	----	----	----	----
Ca	0.425	0.101	0.656	0.001	----	----	----	----	0.002
Ba	----	----	----	----	----	----	----	0.016	0.009
Na	----	0.004	0.002	----	----	----	----	0.013	0.030
K	----	----	----	----	----	----	----	0.857	0.830
Σ cat.	8.007	8.009	8.021	1.000	2.995	1.999	2.999	7.760	6.864

Abbreviations in this and subsequent tables: n.a.= not analyzed, n.d. = not detected; abbreviations of mineral names are after Kretz (1983). In this table all Fe is assumed to be Fe^{2+} except in the case of kyanite, where all is assumed to be Fe^{3+}, and spinel, where Fe^{3+} is calculated using stoichiometric criteria.

examples large enough for quantitative analysis are a group of three *ca.* 50 x 100 μm lamellae of bright blue rutile with common orientation in garnet (specimen DS9315, Table 2) that are high in FeO (0.76 wt%). Elevated TiO_2 and oriented rutile exsolution in pyrope-almandine garnet is well known in mantle xenoliths (Sobolev *et al.*, 1973) and in certain very high-temperature crustal settings and is likely a thermally-controlled phenomenon.

Kyanite

Kyanite is typically very strongly colored, with some examples electric blue or even green in thin section. Blue varieties are notably pleochroic from blue to straw-yellow, with elevated birefringence. Kyanite may contain up to 2.21 wt% Cr_2O_3, 0.63 Fe_2O_3, and 0.22 V_2O_3 and these substituents probably account for the anomalous optical properties (specimen DS9311, Table 2).

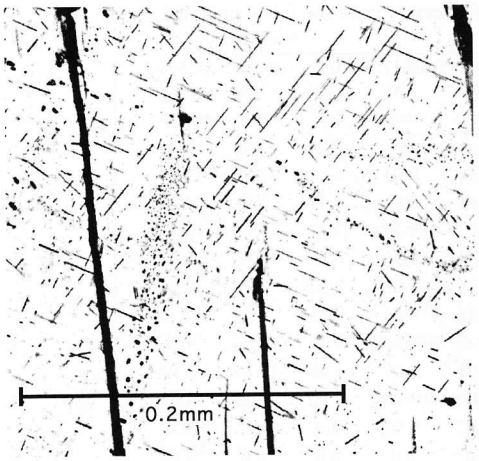

Fig. 5. Rutile needles in garnet, specimen DS9317. The trails of dark spots are planes of fluid inclusions.

Kyanites with Cr_2O_3 locally in excess of 1 wt% are found across the upper deck in quartz-saturated and quartz-undersaturated felsic gneiss, both as inclusions in garnet and free in matrix. This magnitude of substitution of Cr in kyanite is known only from blueschists, eclogites and mantle xenoliths (Kerrick, 1990).

That kyanite should be locally so enriched in Cr in the presence of garnet requires some explanation. Cr_2O_3 contents in kyanite of *ca.* 0.75 to 1.0 wt% are widespread and seem to be in equilibrium with garnet, but examples in excess of 2 wt% are apparently not. These occurences are of two types. The first is rounded green crystals surrounded by plagioclase rims; here the Cr_2O_3 content may have been elevated during resorption. The other examples are from quartz-undersaturated gneisses where heterogeneously-colored kyanite is found together with Cr-corundum and spinel (below) along fractures in large host garnets. Here WDS element-mapping finds an irregular distribution of Cr in these phases in a texture suggesting late Cr-enrichment along the fracture and hence disequilibrium.

Corundum

In the felsic gneiss, corundum is found as large (>1cm) crystals included in garnet and as smaller crystals in feldspathic matrix. The corundum-bearing bands and nodules are 70-90 % garnet whose composition is typically *ca.* $Py_{30}Gr_{20}$. Optical continuity between isolated crystals in garnet suggests that corundum crystals were originally several cm in size and have been extensively replaced by garnet.

Corundum is lavender to violet in hand sample, and in thin section locally colorless to strong pink and pleochroic. Crystals are zoned, with the strongest pink color found adjacent to kyanite, spinel or rutile. A strongly colored corundum (specimen DS9311, Table 2) was found to contain 1.02 wt% Cr_2O_3 and 0.38 Fe_2O_3.

Spinel

Discrete spinel crystals occur only in the quartz-undersaturated gneisses. Their color is green to grey-brown, and they range widely in composition. Significant Zn, Cr and V are usually present (specimen DS9311, Table 2).

Rutile

Rutile is a ubiquitous accessory phase in both matrix and as inclusions in garnet. Rutile in general contains *ca.* 0.5 wt% FeO and 0.1 wt% Cr_2O_3. Some examples contain significant Nb. Crystals are rounded, up to several mm in size and are red-brown or greenish-grey in color.

Large rutile grains from several specimens have been found to contain significant $ZrSiO_4$ as oriented needles in a texture strongly suggestive of exsolution. Two possibilities present themselves. Either a Zr-substituted rutile exsolved its Zr in combination with Si diffusing through its structure, or there was direct exsolution of zircon from a Zr-Si-substituted rutile. This would require minor substituent octahedrally-coordinated Si in the rutile structure. Zr-substitution is well-known in rutile from the upper mantle (Tollo & Haggerty, 1987). Si-substitution in rutile is not as well known, possibly because of the scarcity of suitable (SiO_2-saturated) mantle xenoliths. Published values of SiO_2 in rutile from ultramafic nodules in kimberlite are generally low (0.1-0.3 wt%: Schutze, 1983).

Phlogopite

Phlogopite inclusions in garnet are common. Some are clean pale-brown phlogopite, some are thick with exsolved rutile and/or ilmenite, and others are partially replaced by a symplectite of

K-feldspar + Zn-Cr-rich spinel. Another textural association involves phlogopite found together with quartz + sillimanite intergrowths tangent to garnet and along discolored layer-parallel zones up to several centimeters wide. Sillimanite overgrowths on kyanite are associated with this generation of phlogopite. These zones are interpreted as resulting from granulite-facies retrogression by the re-hydration reaction:

$$Grt + Ksp + H_2O(v \text{ or melt}) = Phl + Sil + Qtz$$

Both relic and late-formed phlogopite show a very wide range in TiO_2 contents, ranging from 0.37 wt% to as much as 3.98 wt% (Table 2), and a narrow range of Mg/(Mg+Fe), 0.75-0.80. Chlorine was not analyzed but in some examples is present in amounts sufficient to be seen on EDS spectra. Garnet-biotite thermometry typically yields calculated temperatures of 600-700°C. This temperature range is so low compared to all other indicators as to indicate complete late reequilibration of phlogopite with garnet. Phlogopite is volumetrically unimportant and therefore is easily overwhelmed during Fe-Mg exchange with the abundant garnet. Hence, little significance for the study of highest metamorphic grade is attached to the phlogopite compositions.

Chlorapatite

Apatite is a fairly common accessory mineral in matrix and is crowded with brown needles several μm thick in an oriented exsolution texture. Qualitative EDS analysis finds the apatite to be very Cl-rich and probably near-endmember chlorapatite. The needles are a light rare earth element-rich phosphate and appear to be monazite. This finding suggests significant solubility of light rare earths in apatite at extreme metamorphic grade.

Monazite

Monazite is found as 0.1-0.5 mm pale green inclusions in garnet. EDS spectra indicate very substantial Th content. Most monazite inclusions in garnet are surrounded by a narrow zone of non-pleochroic brown discoloration of the host. This discoloration is likely due to radiation damage and was probably facilitated by the high Th content in the monazite and at least 2.6 Ga of exposure.

Zircon

Zircon is very common in the matrix of the felsic gneisses and less common as an inclusion in garnet. Zircons are typically large; some reach 0.75-1.00 mm in diameter. Their forms are subhedral and oblate to nearly anhedral and spheroidal (Fig. 6). A complex growth history is apparent, with a typically irregular or broken nucleus, perhaps of detrital origin, overgrown by up to 10-20 concentric subspheroidal inclusion-rich shells. The overgrowths have abundant radial cracks around the nucleii. The overgrowths are intensely fluorescent under the electron beam, and the nucleii much less so. The minor element compositions of the zircons and the identities of their inclusions are presently unknown.

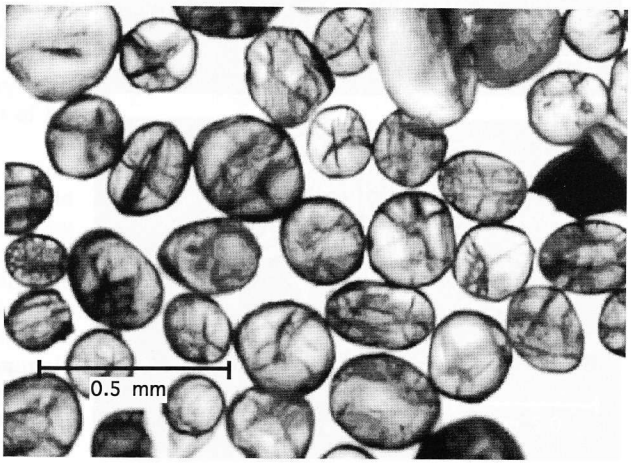

Fig. 6. Zircons, specimen D016. Note the spheroidal form of the metamorphic overgrowths.

Muscovite

Several grains of a highly titanian muscovite have been found in garnet-quartzite M2506. The analysis in Table 2 is an average of eight analyses from a traverse of a fairly homogeneous matrix grain 100 μm in size. Average TiO_2 content in this grain is 4.18 wt% or 0.21 cations pfu. Standard deviation among the eight analyses was 0.53 wt%. MgO is also elevated well beyond normal values, at 1.99 wt% or 0.19 cations pfu (standard deviation 0.19 wt%). The symmetry in Mg and Ti is suggestive of the substitution:

$$Ti^{[6]} + Mg^{[6]} = 2\ Al^{[6]}$$

High-resolution WDS element mapping of the analyzed grain found spatial covariance of Mg and Ti, consistent with the proposed substitution. The Ti-muscovite is not particularly phengitic, at 3.17 Si pfu.

Optically the Ti-rich muscovite is colorless and slightly pleochroic toward pale grey-brown. Relief is noticeably higher than muscovite, and birefringence is also somewhat elevated.

Very similar titanian muscovite, indeed the only other published example of a muscovite near this composition, was reported by Vavilov *et al.* (1993) coexisting with metamorphic diamond in gneisses of the 45-50 kbar, 950-1000°C Kokchetav Massif, northern Kazakhstan. Their highest-Ti muscovite (0.28 Ti and 0.18 Mg pfu) was also notably non-phengitic (Si 3.22 pfu).

The Ti-rich muscovite from the upper deck is found as isolated grains in matrix, *ca.* 75-100 μm in size surrounded by a dark very fine grained material that appears to be graphite, intergrown with fine white mica and scattered 1-2 μm grains of a phase that is bright in BSE and that appears from EDS spectra to be a magnesian ilmenite. Common patches in matrix of a set of phases similar to that rimming the surviving Ti-rich muscovite may record the retrograde decomposition of many other grains. Very similar titanian muscovite is found with graphite included toward the rim of a garnet, without decomposition products.

Experimental work and the description of further natural examples of the Ti-Mg substitution in muscovite will be required before its thermobarometric significance is fully understood. Significantly more phengitic titanian muscovite (Si 3.28-3.37 pfu) has been described from the Brossasco coronite metagranite of the Dora Maira Massif (Biino & Compagnoni, 1992).

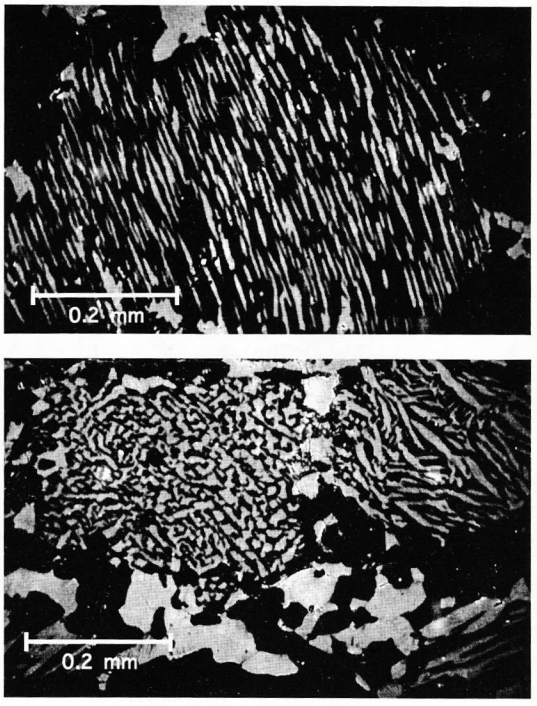

Fig. 7. BSE images of mesoperthites, specimens M249B (top) and M2315 (bottom). The average compositions (Table 3) reported for these two specimens are from these grains.

Ternary feldspars

Feldspars of strongly ternary (Ca, Na, K) composition at highest temperature are found as ribbons with quartz in the matrix of the felsic gneisses and also in many of the associated mafic rocks. The feldspars are mesoperthites, and are now almost completely exsolved into 5-50 μm lamellae, rods and branching networks of K-feldspar, typically *ca.* $An_2Ab_8Or_{89}Cs_1$, in a plagioclase host, *ca.* $An_{29}Ab_{69}Or_2Cs_0$. Minor recrystallization and coarsening of the two components is visible at grain boundaries without measurable compositional changes. Two examples of the mesoperthites are shown in Fig. 7.

In order to homogenize the fine-scale lamellae into an original composition, a method of averaging was employed. Six determinations of homogenized compositions were made on feldspar grains from five specimens (DS9318, M2506, M249B, R77, M2315 [two]). One hundred to one hundred fifty fully quantitative microprobe analyses were done on each grain in a line extending across the traces of the exsolution lamellae using a slightly defocused beam (5-6 μm). The spacing between analytical points was selected as appropriate for the scale of exsolution in the feldspar.

In the analysis of the exsolved feldspars the microprobe calibration could not be optimized for plagioclase or alkali feldspar individually, but had to yield satisfactory results for both. The slightly unsatisfactory nature of the averaged analyses (Table 3) is a result of this requirement. Analyses were filtered for unsatisfactory gross stoichiometry or weight totals, with about 10 % of analyses excluded. Strontium was not analyzed as its presence in any of the specimens could not be verified. Barium is present in various amounts, and on exsolution partitioned strongly into the alkali feldspar component. The presence of barium in some of the ternary feldspars probably reflects the decomposition of biotite earlier in the metamorphic history.

Acceptable analyses were averaged. Representative analyses of the alkali feldspar and plagioclase endmembers were also obtained by averaging. In each case the three determined compositions, two selected endmembers and the bulk average, were strictly collinear meaning that there was no compositional variety beyond the two exsolved components. In the case of sample M2315 two feldspar grains with different exsolution textures were analyzed separately and a nearly identical bulk composition was determined for each, thereby verifying both the analytical method and the assumption of original homogeneity within the ternary feldspar ribbons.

Garnet-clinopyroxenite, Honsvall Lake locality

A minor but very interesting rock type found in several locations in the northern part of the upper deck is a peraluminous kyanite and corundum-bearing garnet-clinopyroxenite with a fassaitic sodian clinopyroxene and an unusually pyropic garnet. This rock is found as layers several meters in thickness that are hosted by quartzofeldspathic gneiss. The garnet-clinopyroxenite bodies are more resistant to erosion than their host rocks and form ridges and promontories. The largest body known is in the northern part of the upper deck, south of Honsvall Lake. This body has been mapped as a sheet up to 15 m thick and traceable along strike for at least 3.5 km.

Table 3. Results of ternary feldspar rehomogenization using a method of averaging of microprobe analyses along traverses of exsolved mesoperthites.

Spec.	M2315a	M2315b	DS9318	M2506	M249B	R77
#pts.	92	91	84	81	120	81
Na_2O	5.45	5.29	5.98	5.21	5.75	5.80
CaO	2.62	2.60	5.18	3.74	3.71	4.01
K_2O	6.36	6.67	3.74	5.75	5.19	4.75
BaO	0.14	0.08	0.29	1.03	0.17	0.46
FeO	0.03	0.03	0.01	0.03	0.05	0.03
Al_2O_3	21.55	21.63	24.06	22.73	22.84	22.71
SiO_2	63.44	63.71	61.52	62.15	62.36	62.07
Total	99.58	100.01	100.78	100.64	100.07	99.83
/8 ox.:						
Na	0.477	0.461	0.517	0.455	0.501	0.507
Ca	0.127	0.125	0.247	0.180	0.179	0.194
K	0.366	0.383	0.213	0.330	0.297	0.273
Ba	0.002	0.001	0.005	0.018	0.003	0.008
Fe	0.001	0.001	0.000	0.001	0.002	0.001
Al	1.147	1.146	1.264	1.206	1.209	1.207
Si	2.864	2.865	2.743	2.799	2.802	2.799
Σ cat.	4.984	4.984	4.990	4.990	4.992	4.988
X:						
Ab	0.49	0.48	0.53	0.46	0.51	0.51
An	0.13	0.13	0.25	0.18	0.18	0.20
Or	0.38	0.39	0.22	0.34	0.31	0.28
Cs	0.00	0.00	0.00	0.02	0.00	0.01

Number of analyses used is shown in the second row of the table.

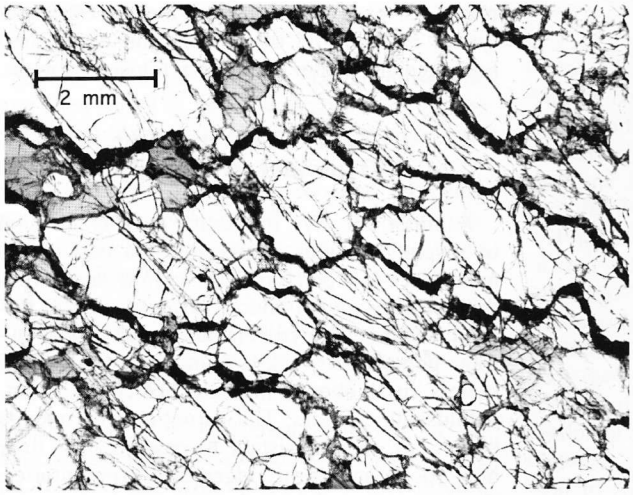

Fig. 8. Garnet-clinopyroxenite from Honsvall Lake, specimen D033E1. Coarse tectonite with garnet and clinopyroxene (pale) and minor pargasite (gray). The dark, thick grain boundaries are kelyphites, and appear to define a penetrative deformational fabric.

Where fresh the rock is a coarse bimineralic tectonite with minor kelyphitization along grain boundaries and fractures within garnet (Fig. 8). Proportions of garnet and sodian clinopyroxene are roughly equal, and their grain sizes range up to 4-5 mm. Pargasite is least abundant in the freshest specimens and is not found included in garnet, as pyroxene is, and is concentrated along garnet-pyroxene grain boundaries. Pargasite therefore may not have been part of the primary mineral assemblage.

Kyanite is a common accessory mineral found only as rounded blades included in garnet. Other accessory minerals are corundum and spinel, found both as inclusions in garnet and free in matrix. Rutile is uncommon and found only as needles in garnet. Piezobirefringent effects (Rosenfeld & Chase, 1961) are observed in thin section around kyanite inclusions in garnet, indicating significant differential expansion between inclusion and host on decompression and cooling.

Analyses of garnet, sodian clinopyroxene and spinel are presented in Table 4. Analyses of corundum and kyanite are not presented, for these are unremarkable in their composition. The major mineral phases are compositionally monotonous and consistent among many specimens suggesting very large-scale primary homogeneity.

Garnets are pink to raspberry-colored and up to 5 mm in size. Many specimens contain garnet aggregates and isolated large garnets in a texture that suggests cataclasis of once-larger garnets (and clinopyroxenes) to produce the present texture. Garnets do not show significant compositional variation across the interiors of large grains. Narrow zones of Fe-Mg exchange are found associated with marginal kelyphites and other symplectites. Pyrope content ranges from Py_{52} to Py_{56} and grossular from Gr_{22} to Gr_{24}. Spessartine is negligible. Sodium, titanium, phosphorus and chromium are at or near detection limits.

Clinopyroxene is very pale apple-green and has in general a smaller grain size than coexisting garnet. Much of the clinopyroxene has a chalky appearance in hand specimen and grains of this type are found to contain abundant Ab_{66} plagioclase in very fine grained lamellar and vermiform textures, with depressed Na in associated clinopyroxene.

The pyroxene is sodian, with generally 2.5-2.7 wt% Na_2O, and is fassaitic, approximately $CaTs_{12}$. Clinopyroxene in retrograde symplectites is even more fassaitic. Mg/(Mg+Fe) is very high, *ca.* 0.87-0.89, and TiO_2 and Cr_2O_3 are low. All Fe is considered as Fe^{2+} in the analysis in Table 4. Coexisting spinel is fully aluminous and evidently has little ferric iron, and coexisting pargasite has a stoichiometry that does not imply the existence of much ferric iron in that mineral either. If there were significant ferric iron in this system it would be expected to partition strongly into the spinel and the amphibole.

Retrograde effects

Discrete crosscutting veins and diffuse patches

Table 4. Selected mic
garnet-clinopyroxenit

Spec.	DS9322	DS
	Cpx	
SiO_2	51.99	4
TiO_2	0.13	
Al_2O_3	8.91	1
Cr_2O_3	0.02	
MgO	12.88	1
FeO	2.86	
MnO	0.02	
CaO	20.72	1
ZnO	n.a.	
Na_2O	2.68	
K_2O	n.d.	
Total	100.21	9
N ox.:	6	
Si	1.875	6.
Ti	0.004	0.
Al	0.379	2.
Cr	0.001	
Mg	0.692	3.
Fe	0.086	0.
Mn	0.001	0.
Ca	0.801	1.
Zn	-----	
Na	0.187	0.
K	-----	0.
Σ cat.	4.026	15.

of leucocratic mater
pyroxenite. Euhedra
are found at the selv
of the veins. Smal
clinopyroxene are p
the pargasite megacr
these leucocratic seg
are melts, and the p
nate.

The garnet-clinopy
ified by extensive r
fractures and by mo
roxene contacts by a
+ plagioclase + orth
symplectites of plag
clinopyroxene or p
poraneous with lo
clinopyroxene and p
and An_{66} plagioclase

The contacts betw

Table 4. Selected microprobe analyses of minerals from garnet-clinopyroxenite, Honsvall Lake locality.

Spec.	DS9322	DS9322	DS9322	M2319A	M2319A
	Cpx	Prg	Grt	Grt	Spl
SiO_2	51.99	42.80	41.53	41.12	0.10
TiO_2	0.13	0.32	0.02	0.02	0.02
Al_2O_3	8.91	15.07	23.79	23.49	67.53
Cr_2O_3	0.02	n.d.	0.03	0.04	0.08
MgO	12.88	17.11	14.76	14.88	19.64
FeO	2.86	5.22	11.21	13.81	12.73
MnO	0.02	0.01	0.24	0.33	n.d.
CaO	20.72	12.14	9.05	6.68	n.d.
ZnO	n.a.	n.a.	n.a.	n.a.	0.12
Na_2O	2.68	2.89	0.01	n.a.	n.a.
K_2O	n.d.	0.89	n.a.	n.a.	n.a.
Total	100.21	96.45	100.64	100.37	100.22
N ox.:	*6*	*23*	*12*	*12*	*4*
Si	1.875	6.192	2.994	2.990	0.002
Ti	0.004	0.034	0.001	0.001	-----
Al	0.379	2.569	2.021	2.013	1.994
Cr	0.001	-----	0.002	0.002	0.002
Mg	0.692	3.690	1.586	1.614	0.733
Fe	0.086	0.632	0.676	0.521	0.267
Mn	0.001	0.001	0.015	0.020	-----
Ca	0.801	1.882	0.699	0.840	-----
Zn	-----	-----	-----	-----	0.002
Na	0.187	0.811	0.001	-----	-----
K	-----	0.164	-----	-----	-----
Σ cat.	4.026	15.975	7.995	8.001	3.000

of leucocratic material are found in the garnet-pyroxenite. Euhedral 1-3 cm pargasite crystals are found at the selvages and free in the interiors of the veins. Small remnants of garnet and clinopyroxene are poikiloblastically enclosed in the pargasite megacrysts. The texture and style of these leucocratic segregations suggest that they are melts, and the pargasite appears to be cognate.

The garnet-clinopyroxenite is otherwise modified by extensive replacement of garnet along fractures and by modification of garnet-clinopyroxene contacts by a μm-scale kelyphite of spinel + plagioclase + orthopyroxene. Texturally later symplectites of plagioclase and orthopyroxene, clinopyroxene or pargasite are penecontemporaneous with local breakdown of sodian clinopyroxene and production of sodian augite and An_{66} plagioclase.

The contacts between the garnet-clinopyroxenite and its quartzofeldspathic host gneisses are locally decorated with a bright blue sapphirine bearing rock with pink to orange-colored garnets. The sapphirine diminishes in abundance away from the garnet-clinopyroxenite and vanishes in less than 1 m. The sapphirine-bearing rock apparently originally consisted of garnet, kyanite and clinopyroxene with abundant quartz ribbons. Up to 60-70 % of the volume of the rock now consists of symplectites of anorthite + sapphirine, anorthite + corundum, plagioclase + spinel and plagioclase + orthopyroxene with the remainder consisting of relic garnet, kyanite and quartz. Study of the rich variety of symplectites in the garnet-pyroxenite and in the sapphirine bearing rock is expected to constrain the retrograde P-T path of the upper deck with considerable detail, provided adequate allowance can be made for the evidently very small scale of domainal equilibrium.

Thermobarometry

Garnet-clinopyroxenite

Garnet and clinopyroxene compositions reported from specimen DS9322 in Table 4 are interior compositions of adjacent crystals that are known from quantitative compositional traverses and X-ray mapping to be homogeneous and representative of the specimen. There is no evidence of disequilibrium between these phases. Application of garnet-clinopyroxene thermometry to this pair finds 980°C (Ellis & Green, 1979) or 970°C (Krogh, 1988) at a reference pressure of 15 kbar.

Here the matter of possible ferric iron in the pyroxene becomes pressing. Recalculation of the pyroxene formula based on stoichiometry dramatically lowers the calculated temperature because of the very low total iron, and consequently large changes in $Mg/(Mg+Fe^{2+})$. Formula recalculation proceeding from stoichiometry alone may also assume too much analytical accuracy for all other analyzed components, most particularly Si and Al. The garnet-clinopyroxene thermometer of Berman *et al.* (1995) proceeds with the instruction that all Fe be considered as Fe^{2+} unless there is evidence that the mineral assemblage is highly oxidized, thereby allowing for the likely presence of minor Fe^{3+} in experimental and natural calibrants. Application of this thermometer finds 950°C at 15 kbar. Because of the facility of Fe-Mg exchange

in this system, these calculated temperatures probably reflect some resetting of exchange equilibria during cooling.

The presence of corundum with clinopyroxene and a garnet of this composition indicates a minimum pressure of 15 kbar if at a temperature of 950-1000°C (Gasparik, 1984). The primary mineral phases afford little other opportunity for barometry.

Ternary feldspar thermometry

The six homogenized ternary feldspar compositions from Table 3 allow a determination of minimum peak metamorphic temperature. In Fig. 9 these recovered compositions are plotted on an An-Ab-Or ternary diagram in relation to the ternary feldspar solvus calculated at 1000° and 1100°C at a reference pressure of 15 kbar according to the model of Fuhrman & Lindsley (1988). All compositions are above the 1000°C solvus and some approach the 1100°C solvus. A reference pressure of 15 kbar was selected because many of the ternary feldspars coexist with kyanite, providing a lower pressure limit in the 1000° to 1100°C temperature range.

Ternary feldspar thermometry is most commonly applied in igneous systems containing two coexisting feldspars which are on a solvus and can therefore yield a fairly exact determination of temperature (Fuhrman & Lindsley, 1988). No evidence for two coexisting equilibrium feldspars in the matrix has been seen here. The determined temperature is therefore only a minimum, as it is the lowest temperature required for the existence of the given feldspar as a homogeneous mineral. This is true regardless of whether it is on a solvus as one of an equilibrium pair, or is a single hypersolvus phase. The recovered ternary compositions are near the critical composition in the temperature range of interest and so if these feldspars were but one of a pair of phases on a solvus, their companion feldspars would not have differed greatly in composition.

The ternary feldspar solvus is relatively insensitive to pressure. Slight changes in solvus positions at 1000° and 1100°C calculated for 10 kbar and 20 kbar (not shown) do not affect the conclusion of this homogenization study, that strongly ternary feldspars from felsic gneisses across the upper deck cannot have existed as single homogeneous phases at a temperature less than 1000°C at any pressure. The mixing lines between endmember exsolved compositions (alkali = *ca.* Or_{88}-Or_{96}, plagioclase = *ca.* An_{22}-An_{32}) are subparallel to the ternary feldspar solvus in the region of interest. Therefore, possible minor errors in sampling the proportions of the endmembers would shift the homogenized compositions slightly along a mixing line and also not affect the conclusions.

In quartzofeldspathic rocks, ternary feldspars of compositions similar to these may only be found in nearly anhydrous settings, because the

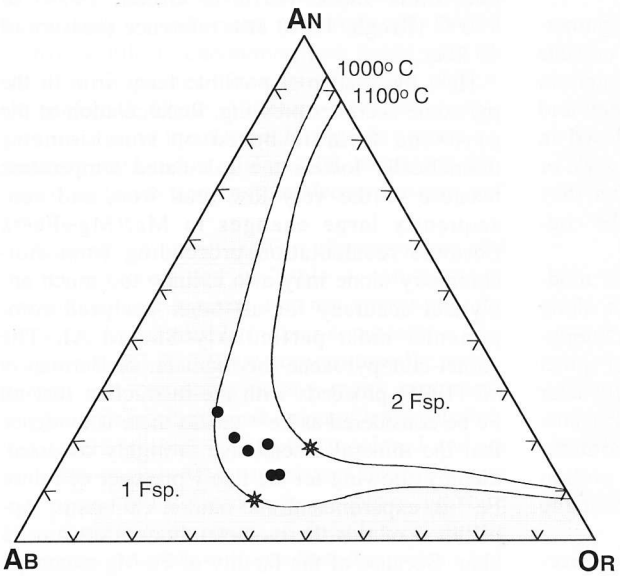

Fig. 9. Feldspar compositions from Fig. 3 (dots), plotted in relation to the ternary solvi and critical compositions (stars) at 1000°C and 1100°C, 15 kbar according to the model of Fuhrman & Lindsley (1988) and calculated with the assistance of the MTHERM3 program by those authors.

temperatures they require are far above those for typical feldspar-quartz hydrous melts. Their widespread presence in the felsic gneisses of the upper deck is consistent with the extreme scarcity of hydrous minerals in these rocks.

Barometry of felsic gneiss

The widespread association of > 1000°C ternary feldspar ribbons and kyanite in matrix establishes a minimum metamorphic pressure of *ca.* 15 kbar, an unusually high temperature and pressure part of the granulite facies. No unambiguous evidence for pressure in excess of this has been found. One might not expect such evidence to be preserved in matrix in such a high-temperature, high-strain environment. However, included in garnets from felsic gneisses across the upper deck are polyphase kyanite + quartz + Na-K-feldspar assemblages in calcic garnet and these may indicate a somewhat more advanced pressure.

An example of one of these inclusions from a well-studied garnet from specimen M2506 is shown in Fig. 10. Three kyanites, one containing a calcic garnet inclusion are associated with quartz and appear to have once been embayed in a single alkali feldspar that does not contain a detectable anorthite component. Crystallographic continuity is shown by common orientation of string perthite in isolated parts of the now-exsolved alkali feldspar. The two components of the perthite are *ca.* $Or_{56}Ab_{44}$ and $Or_{88}Ab_{12}$. Plagioclase (An_{36} in the illustrated example) is found as rims between and among all phases and is associated with a steep decline in grossular content of the host garnet adjacent to the rims (see next section). These textural and compositional observations are repeated in many examples of this included assemblage from many localities. At high metamorphic grade there was evidently regional development of mineral assemblages involving kyanite, calcic garnet and quartz without plagioclase. This suggests instability of the anorthite molecule at the highest grade. A corollary to this conclusion is that the anorthite component of the ternary feldspars in matrix may also be of retrograde origin, its calcium having been stored as grossular component in garnet at higher pressures.

Determination of the position of the plagioclase-out 'GASP' (Garnet-Aluminosilicate-Silica-Plagioclase) reaction (Koziol & Newton, 1988) is very sensitive to choice of activity-composition models for garnet and feldspar, and in any case requires that these models be extended beyond their demonstrated applicability. Therefore no attempt is made to estimate a higher pressure than the 15 kbar indicated by the presence of kyanite at 1000°C.

Ca-zonation in garnet

Garnets in the felsic gneisses contain profound Ca-zonation. Fig. 11 (a) is an optical image of a *ca.* 5.5 mm diameter garnet from specimen M2506. The included assemblages in this garnet and its Ca-zoning patterns are typical of garnets in the felsic gneisses of the upper deck. This garnet hosts the polyphase inclusion shown in Fig. 10, and has received fairly intensive study.

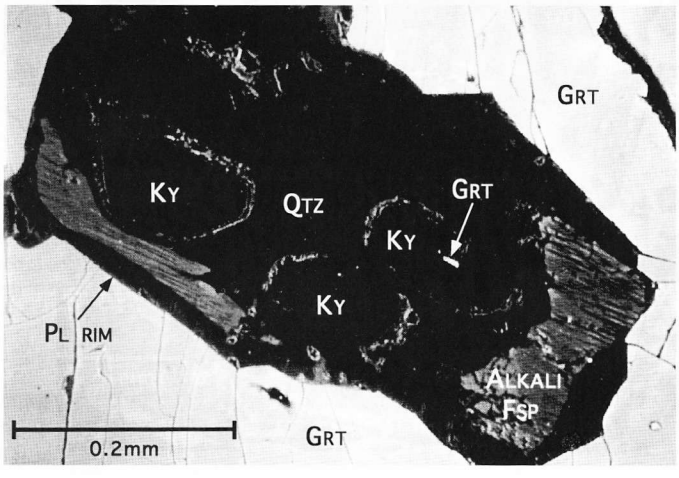

Fig. 10. A polyphase kyanite + quartz + alkali feldspar inclusion in garnet, specimen M2506. Note the crystallographic continuity of the alkali feldspar and the presence of plagioclase as rims.

Fig. 11 (b) is a wavelength-dispersive X-ray map of Ca$K\alpha_1$ in the same field of view as the optical image. The experimental conditions are presented in the figure caption. Ca-zonation is obviously of large magnitude but is smooth, even and continuous. A near-marginal rim of high Ca content falls steeply away outboard toward matrix, and much more shallowly inwards toward a relatively flat interior plateau. Around polyphase (kyanite-quartz-alkali feldspar) inclusions are broad swells in Ca content dropping steeply down immediately adjacent to the inclusions.

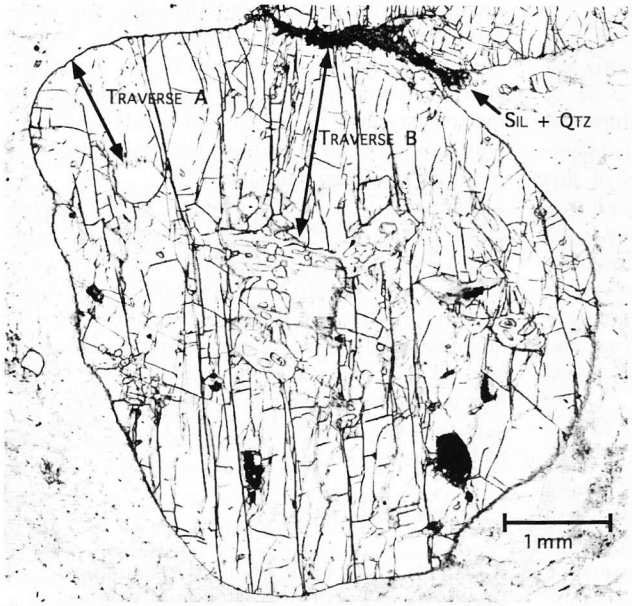

a

b

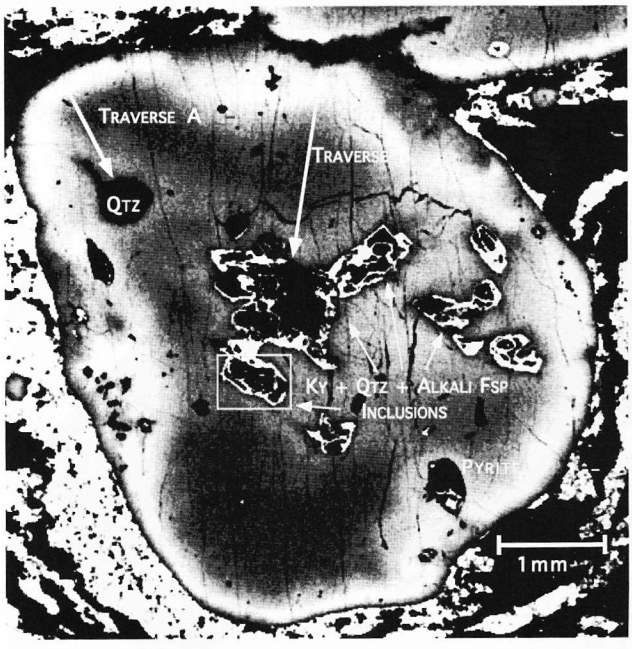

Fig. 11. **(a)** Optical image of a garnet from specimen M2506. The polyphase inclusion illustrated in Fig. 13 is visible in the lower center, along with several others of identical mineralogy. The matrix consists of ternary feldspar and quartz ribbons with minor discrete plagioclase adjacent to the garnet. Lines are locations of two quantitative compositional traverses (A and B of Fig. 12).

Fig. 11. **(b)** Wavelength-dispersive X-ray map of Ca$K\alpha_1$, same field of view as Fig. 11 (a). Size is 1024 x 1024 pixels, pixel size 6 μm. Beam current was 45 nA, counting time 70 ms per pixel, spot size *ca.* 5 μm. Lighter grays are the highest intensities. Many polyphase Ky + Qtz + alkali Fsp inclusions are visible. The white frame shows the area in Fig. 10. Note the development of plagioclase (bright) rims between and among the phases in these inclusions, and the associated depletion of Ca in the adjacent garnet.

Plagioclase rims on the mineral grains in the inclusions are conspicuous in this view.

Two fully quantitative analytical traverses were run along the lines shown in Fig. 11 (a) and results are plotted in Fig. 12. Traverse A contains 165 points and runs from a quartz inclusion across a plateau of Gr_7 and up and over a marginal rim of high Ca content, peaking at Gr_{15} and dropping to Gr_4 at the rim. The perturbations in Fe and Mg visible in the profile are the locations

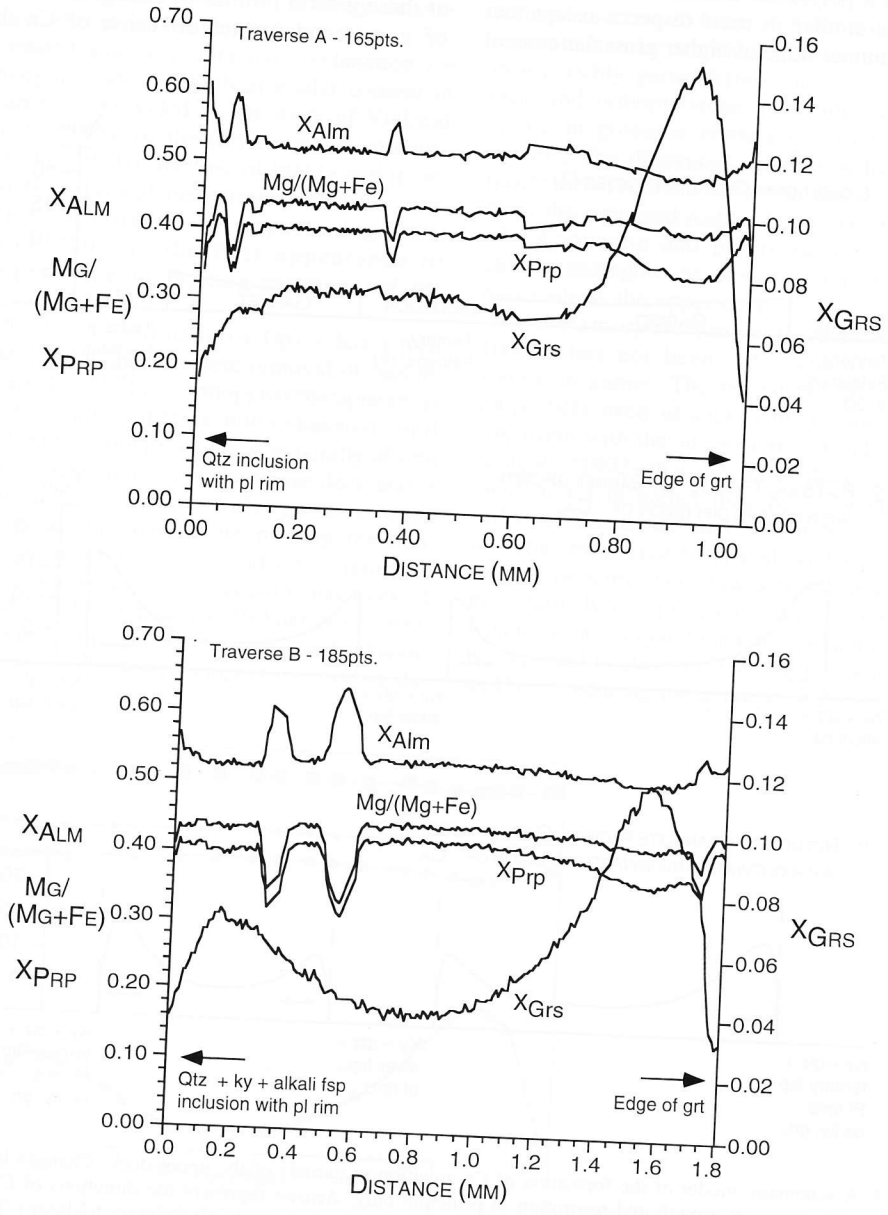

Fig. 12. Analytical traverses of garnet shown in Fig. 11 (a). Traverse A crosses from a quartz inclusion out to the rim, and traverse B from a polyphase inclusion to the rim. The scale for X_{Alm}, Mg/(Mg+Fe), and X_{Prp} is shown on the left, and that for X_{Grs} on the right.

of fractures along which there has evidently been retrograde reequilibration with another ferromagnesian phase. This phase is probably phlogopite which forms a small part of this specimen. Notably, the Ca-profile is undisturbed across these fractures. Traverse B, 185 points, runs from a polyphase inclusion to the garnet's rim and is similar in most respects except that there is an inner ridge of higher grossular content clearly symmetrical to the outer ridge but of smaller magnitude (Gr_6).

These profiles are interpreted as recording (1) the breakdown of plagioclase and the growth of higher-Ca garnet and synchronous inward diffusion of Ca under conditions of increasing pressure or isobaric cooling, and (2) the modification of these growth profiles by retrograde resorption of garnet and further diffusion of Ca during

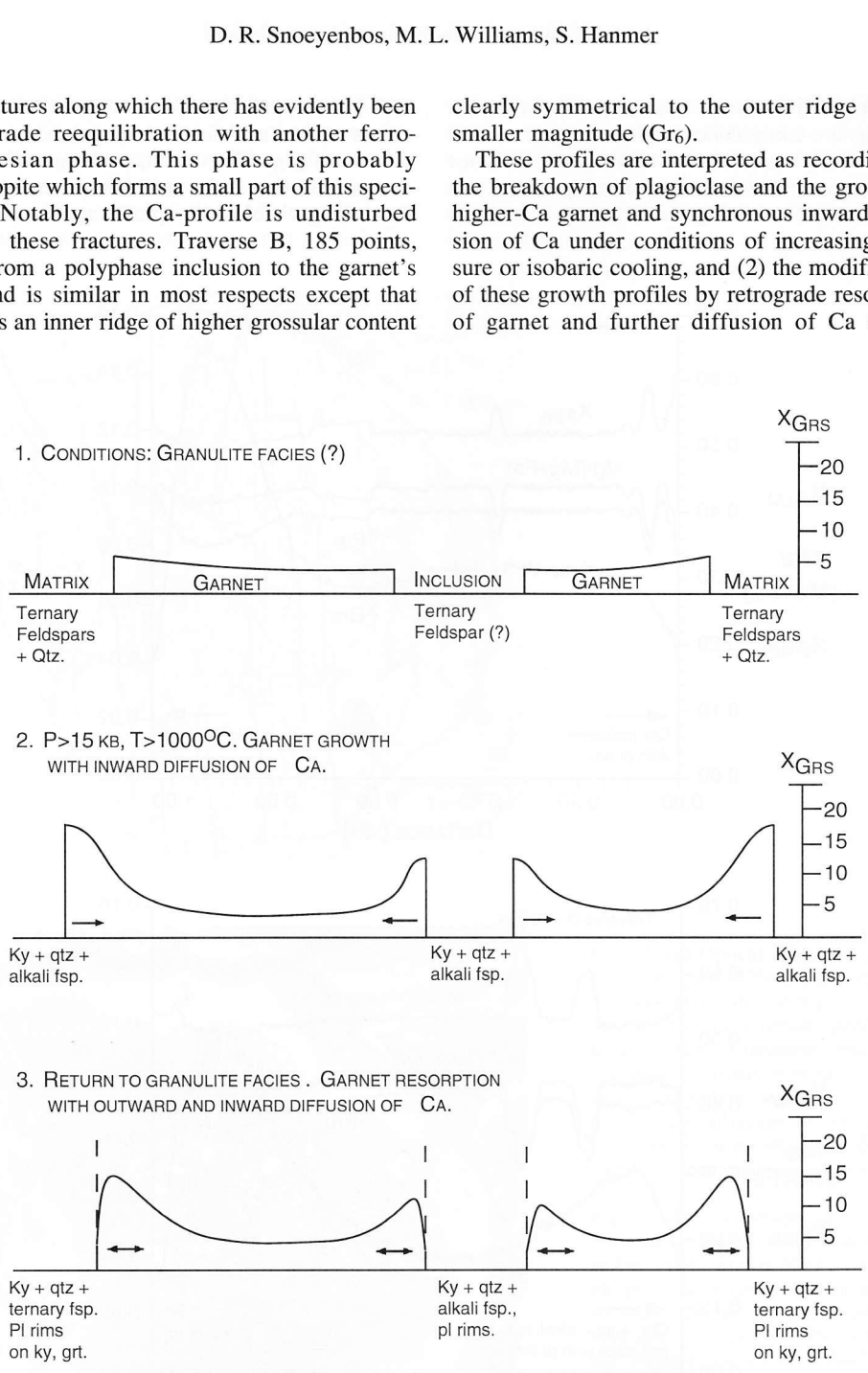

Fig. 13. A schematic model of the formation of Ca-zonation in garnets of the upper deck. Changes in the width of the garnet represent growth and resorption in principle only. Arrows represent the directions of Ca-diffusion. **a)** An original, granulite-facies (?) garnet of moderate grossular content, containing ternary feldspar (?) inclusions. **b)** At elevated pressure, successively higher-Ca garnet grows both outside from matrix and inside around an original feldspar inclusion. **c)** During return to lower-crustal conditions, garnet is resorbed. Diffusional relaxation of zoning profiles occurs throughout the process.

decompression and reconstitution of plagioclase. The albite component of the internal plagioclase rims is interpreted as having diffused from the alkali feldspar during plagioclase growth. A schematic model of this process is presented in Fig. 13. Some aspects of this model would also be satisfied by some amount of isobaric cooling from *ca.* 15 kbar, 1000°C followed by decompression, still at very high temperature

A related and very attractive explanation for the marginal ridge of high grossular content in the garnets is provided by the work of Vielzeuf & Montel (1994) on the partial melting of metagreywackes. Partial melting of biotite and its removal from typical metagreywacke bulk compositions involves two important general reactions. One is the first appearance of ortho-pyroxene in melting-reactions of the general form:

Bt + Pl + Qtz = Grt(Crd,Spl) + Opx + Kfs + melt

and the other is the complete removal of biotite. For example, at 6 kbar orthopyroxene appears at *ca.* 825°C and biotite is not exhausted until nearly 900°C. Orthopyroxene is generally absent from the felsic gneisses of the upper deck and if it had been generated in an early, granulite-facies stage by this familiar biotite melting reaction, some explanation must be found for its removal. However, according to the experimental work of Vielzeuf and Montel, above 16 kbar at *ca.* 900-950°C the biotite-out reaction curves backward and crosses to the lower-temperature side of the orthopyroxene-in reaction. Abundant garnet of *ca.* Gr_{15} is produced in experimental runs at 20 kbar, 850°C and biotite is removed from the assemblage without the formation of orthopyroxene. If the felsic gneisses were originally biotite-rich Al-metagreywackes, then vapor-absent melting of biotite during an excursion to somewhat above 15 kbar, 1000°C might produce a restite similar to what is seen: nearly anhydrous, richly garnetiferous gneisses without biotite and orthopyroxene and with profound increase in grossular content toward the rims of garnets. The illustrated example is from a very quartz-rich rock and differs in that respect only from the proposed restite. However, its patterns of Ca-zonation and polyphase inclusions are closely analogous to those in more feldspathic rocks across the upper deck.

A metamorphic temperature in excess of 1000°C has not been sufficient to erase Ca-zoning in garnet. The persistence of prominent Ca-profiles even at such a high temperature is consistent with the suggestion by Chakraborty & Ganguly (1992) that the tracer diffusion coefficient of Ca in garnet may be as much as two orders of magnitude smaller than that of Fe. Factors that may have further slowed Ca-diffusion include pressure, very low activity of H_2O, and the relatively pyropic composition of the garnet, which on basic crystal-chemical principles would be expected to slow diffusion of larger ions such as Ca by reducing the average cell dimensions.

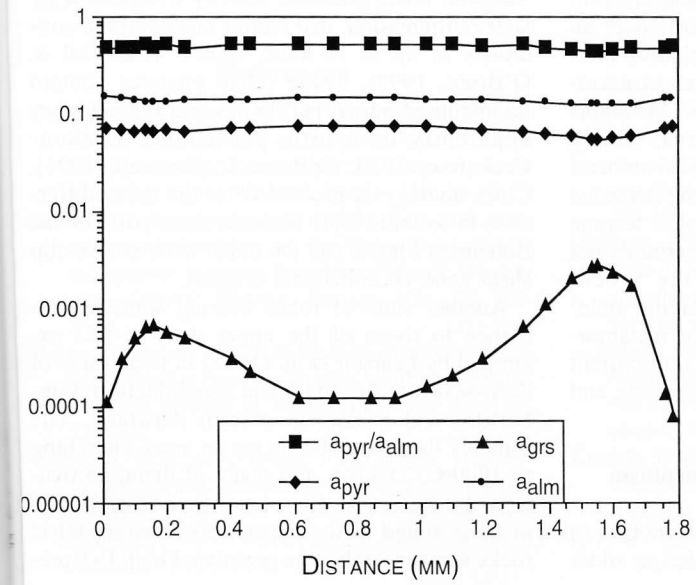

Fig. 14. Twenty representative points from Traverse B, with activities of Alm. Prp and Grs calculated at 1000°C using the activity coefficients of Newton & Haselton (1981).

The compositional profiles in Fig. 12 show a number of other remarkable features. Despite a large change in grossular content in these profiles, the Mg/(Mg+Fe) ratio remains nearly constant, except for a slight antithetic covariance with Grs visible across the higher peaks. A drop in Mg/(Mg+Fe) with increasing Ca would be consistent with ternary mixing effects in garnet (Ganguly & Saxena, 1984). The relatively constant Mg/(Mg+Fe) of this garnet across steep topography of Grs, and the slight drops in Mg/(Mg+Fe) with higher Grs imply that Mg and Fe, more mobile elements, have maintained constant activity at changing mole fraction and slightly changing relative concentrations by diffusing through and past a steep and relatively fixed compositional gradient in Ca. This is also verified by calculation of activities of Grs, Prp and Alm using the activity coefficients of Newton & Haselton (1981) and a temperature of 1000°C. Estimates of the activities of these three components for twenty representative points from traverse B are presented in Fig. 14. To a first approximation, not even including a propagation of likely analytical error through the activity calculation, it appears that Prp and Alm maintain constant activities as Fe and Mg interdiffuse past Ca.

Discussion

Examination of felsic gneiss and gneiss-hosted metabasite finds evidence for metamorphic conditions of at least 15 kbar and 1000°C over an area of 400 km^2. Independent quantitative thermometric and barometric indicators show excellent agreement in several rock types. Metamorphic assemblages, reaction textures, zoning patterns in porphyroblasts and unusual mineral compositions are all consistent with the indicated conditions. That such a metamorphic terrane should exist is perhaps welcome but certainly not surprising information, given the recent enormous expansion of the P-T 'playing field' for crustal petrology. That the age of metamorphism be Archean, and the setting a transcurrent intracontinental shear zone, poses surprising and difficult problems.

Antiquity of high-pressure metamorphism

High-pressure metamorphism has not been found in crustal settings reliably dated as older than late Middle Proterozoic, *ca.* 1.0-1.1 Ga (Sanders *et al.*, 1984). Two possible examples of older eclogites are known, and neither is well-preserved. Rocks interpreted as highly retrograded Early Proterozoic *ca.* 1.85-2.0 Ga eclogites have been found in South-East Greenland (Messiga *et al.*, 1990). Similar rocks are known from the Aldan Shield, Siberia and also are not older than Early Proterozoic, *ca.* 2.4 Ga at most (Smelov & Beryozkin, 1993). Both of these examples involve evidence for a medium-temperature eclogite-facies history found in isolated and highly retrograded mafic rocks, and bear no resemblance to the HT-HP acid granulites and other rocks of the upper deck.

The age of the metamorphism of the upper deck is not known. What is known is only its Late Archean age of juxtaposition against the lower-crustal granulite-facies mylonites of the lower deck, 2.62-2.59 Ga. Knowledge of the age of the metamorphism itself would be extremely useful both in understanding the assembly of the several lithotectonic domains of the East Athabasca mylonite triangle, and in expanding the range of tectonic processes known to have operated in the Archean.

Analogous rocks?

There are two published examples of rocks that may have some affinity to the upper deck. The Bohemian Massif contains small packages of Variscan felsic gneisses, heavily overprinted by later retrogression, that record metamorphic conditions of up to 16 kbar, 1000°C (Carswell & O'Brien, 1993). These felsic gneisses contain fragments of garnet peridotites and HT eclogites apparently of mantle provenance (Bakun-Czubarow, 1983; O'Brien & Carswell, 1994). Close analogy is precluded by the great difference in tectonic style between these parts of the Bohemian Massif and the upper deck (strike-slip shear zone *vs.* collisional orogen).

Another suite of rocks bearing some resemblance to those of the upper deck is that examined by Pearson *et al.* (1991) in their study of deep-seated mafic and felsic xenoliths from kimberlites and basalts in eastern Australia. The samples they describe lie on an array stretching to 1000°C, 21 kbar, and many of them, particularly the mafic coronites, bear close resemblance to those found in the upper deck. Among felsic rocks some resemble the postulated high P-T pre-

cursors to the felsic gneisses. These rocks serve as a reminder that felsic crustal materials may form a significant component of subcontinental lithosphere. The upper deck is possibly a sample of such materials elevated somehow into the lower crust in a heterogeneous intracontinental strike-slip shear zone.

The upper deck presents unusual tectonic and petrologic problems, that connect to large questions of continental evolution, deep cratonic structure, and tectonic processes in 'deep time'. Elevation of the upper deck and its juxtaposition with lower-crustal granulites occurred within a transcurrent intracontinental shear zone, an environment not known to exhume high-pressure rocks; further, this happened in the Late Archean, a time in Earth history from which very high pressure crustal rocks are not otherwise known.

Acknowledgements: The authors are grateful to the many petrologists who have helped them to navigate in little-travelled regions. In particular, this paper has benefitted from the careful attention and constructive reviews of T. Carswell, S. Harley and C. Chopin. Thanks also are extended to Chris Kopf for key insights in the field, and to Mark Darrach for finding the Honsvall Lake locality. This work has been supported by National Science Foundation grants EAR-916001 and EAR- 9406443 to M.L.W., and by the continued generosity of the Geological Survey of Canada. This paper is GSC contribution number 15295.

References

Berman, R.G., Aranovich, L.Ya., Pattison, D.R.M. (1995): Reassessment of the garnet-clinopyroxene Fe-Mg exchange thermometer: II. Thermodynamic analysis. *Contrib. Mineral. Petrol.*, **119**, 30-42.

Biino, G.G., Compagnoni, R. (1992): Very-high pressure metamorphism of the Brossasco coronite metagranite, southern Dora Maira Massif, Western Alps. *Schweiz. Mineral. Petrogr. Mitt.*, **72**, 347-363.

Bakun-Czubarow, N. (1983): Mineral chemistry of garnet lherzolites from the Sudetes, southwest Poland. Carnegie Institute of Washington, Year Book 82, 336-343.

Carswell, D.A. & O'Brien, P.J. (1993): Thermobarometry and geotectonic significance of high-pressure granulites: examples from the Moldanubian zone of the Bohemian Massif in lower Austria. *J. Petrol.*, **34**, 427-459.

Chakraborty, S. & Ganguly, J. (1992): Cation diffusion in aluminosilicate garnets: experimental determination in spessartine-almandine diffusion couples, evaluation of effective binary diffusion coefficients, and applications. *Contrib. Mineral. Petrol.*, **111**, 74-86.

Cumming, G.L. & Krstic, D. (1992): The age of unconformity related uranium mineralization in the Athabasca Basin, northern Saskatchewan. *Canad. J. Earth Sci.*, **29**, 1623-1639.

Ellis, D.J. & Green, E.H. (1979): An experimental study of the effect of Ca upon garnet-clinopyroxene Fe-Mg exchange equilibria. *Contrib. Mineral. Petrol.*, **71**, 13-22.

Fuhrman, M.L. & Lindsley, D.H. (1988): Ternary-feldspar modeling and thermometry. *Am. Mineral.*, **73**, 201-215.

Ganguly, J. & Saxena, S.K. (1984): Mixing properties of aluminosilicate garnets: constraints from natural and experimental data, and applications to geothermo-barometry. *Am. Mineral.*, **69**, 88-97.

Gasparik, T. (1984): Experimentally determined stability of clinopyroxene + garnet + corundum in the system CaO-MgO-Al_2O_3-SiO_2. *Am. Mineral.*, **69**, 1025-1035.

Hanmer, S. (1994): Geology, East Athabasca mylonite triangle, Stony Rapids area, northern Saskatchewan. Geological Survey of Canada, Map 1859A, scale 1:100,000.

Hanmer, S., Darrach, M., Kopf, C. (1992): The East Athabasca mylonite zone: an Archean segment of the Snowbird tectonic zone in Northern Saskatchewan. *Current Research, Part C*, Geological Survey of Canada, Paper **92-1C**, 19-29.

Hanmer, S., Parrish, R., Williams, M., Kopf, C. (1994): Striding-Athabasca mylonite zone: Complex Archean deep crustal deformation in the East Athabasca mylonite triangle, northern Saskatchewan. *Canad. J. Earth Sci.*, **31**, 1287-1300.

Hanmer, S., Williams, M.L., Kopf, C. (1995): Striding-Athabasca mylonite zone: implications for the Archean and Early Proterozoic tectonics of the western Canadian Shield. *Canad. J. Earth Sci.*, **32**, 178-196.

Hoffman, P.F. (1988): United plates of America, the birth of a craton: Early Proterozoic assembly and growth of Laurentia. *Ann. Review Earth Planet. Sci.*, **16**, 543-603.

— (1989): Precambrian geology and tectonic history of North America. *in* "The Geology of North America - an overview", A.W. Bally, A.R. Palmer, eds. Geological Society of America, Boulder, 447-512.

Kerrick, D.M. (1990): The Al_2SiO_5 polymorphs. *Reviews in Mineralogy 22*, Mineralogical Society of America, 406 p.

Koziol, A.M. & Newton, R.C. (1988): Redetermination of the anorthite breakdown reaction and an im-

provement of the plagioclase-garnet-Al_2SiO_5-quartz geobarometer. *Am. Mineral.*, **73**, 216-223.

Kretz, R. (1983): Symbols for rock-forming minerals. *Am. Mineral.*, **68**, 277-279.

Krogh, E.J. (1988): The garnet-clinopyroxene Fe-Mg geothermometer - a reinterpretation of existing experimental data. *Contrib. Mineral. Petrol.*, **99**, 44-48.

Messiga, B., Tribuzio, R., Vannucci, R. (1990): Mafic and ultramafic pods with eclogitic relics from the Proterozoic Nagssugtoquidian mobile belt of East Greenland. *Lithos*, **25**, 101-118.

Newton, R.C. & Haselton, H.T. (1981): Thermodynamics of the garnet-plagioclase-Al_2SiO_5-quartz geobarometer. *in* "Thermodynamics of minerals and melts", R.C. Newton, A. Navrotsky and Wood, B.J., eds. Springer-Verlag, New York, 131-147.

O'Brien, P.J. & Carswell, D.A. (1994): Tectonometamorphic evolution of the Bohemian Massif: evidence from high pressure metamorphic rocks. *Geol. Rundschau*, **82**, 531-555.

Pearson, N.J., O'Reilly, S.Y., Griffin, W.L. (1991): The granulite to eclogite transition beneath the eastern margin of the Australian craton. *Eur. J. Mineral.*, **3**, 293-322.

Rosenfeld, J.L. & Chase, A.B. (1961): Pressure and temperature of crystallization from elastic effects around solid inclusions in minerals? *Amer. Jour. Sci.*, **259**, 519-541.

Sanders, I.S., van Calsteren, P.W.C., Hawkesworth, C.J. (1984): A Grenville Sm-Nd age for the Glenelg eclogite in north-west Scotland. *Nature*, **312**, 439-440.

Schutze, D.J. (1983): Graphic rutile-olivine intergrowths from South African kimberlites. Carnegie Institute of Washington, Year Book 82, 343-346.

Smelov, A.P. & Beryozkin, V.I. (1993) : Retrograded eclogites in the Olekma granite-greenstone region, Aldan Shield, Siberia. *Precambrian Research*, **62**, 419-430.

Sobolev, N.V., Lavrent'ev, Yu. G., Pospelova, L.N., Pokhilenko, N.P. (1973): Isomorphic titanium admixture in pyrope-almandine garnets [in Russian], *Zapiski Vsesoyuznogo Mineralogicheskogo Obschestva*, **102**, no. 2.

Thomas, M.D., Grieve, R.A.F, Sharpton, V.L. (1988): Gravity domains and assembly of the North American continent by collisional tectonics. *Nature*, **331**, 333-334.

Tollo, R.P. & Haggerty, S.E. (1987): Nb-Cr rutile in the Orapa kimberlite, Botswana. *Can. Mineral.*, **25**, 251-264.

Vavilov, M.A., Sobolev, N.V., Shatskiy, V.S. (1993): Micas in diamond-bearing metamorphic rocks of northern Kazakhstan. Akademiia Nauk SSSR, *Doklady Earth Sciences Section*, **319A(6)**, 177-182.

Vielzeuf, D. & Montel, J.M. (1994): Partial melting of metagreywackes. Part 1. Fluid-absent experiments and phase relationships. *Contrib. Mineral. Petrol.*, **117**, 375-393.

Williams, M.L., Hanmer, S., Kopf, C. (1995): Syntectonic generation and segregation of tonalitic melts from amphibolite dikes in the lower crust, Chipman dike swarm, northern Saskatchewan. *J. Geophys. Research*, in press.

Received 20 February 1995
Accepted 21 June 1995